AD-A136 502 PRELIMINARY ANALYSIS OF RESULTS OF A MOUNTAIN AREA ATMOSPHERIC DIFFUSION TEST(U) FOREIGN TECHNOLOGY DIV WRIGHT-PATTERSON AFB OH 08 DEC 83 FTD-ID(RS)T-1637-83 1/1

UNCLASSIFIED F/G 13/2 NL

END
DATE FILMED
1 84
DTIC

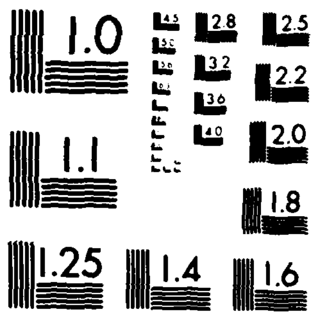

MICROCOPY RESOLUTION TEST CHART
NATIONAL BUREAU OF STANDARDS 1963 A

(2)

FTD-ID(RS)T-1637-83

FOREIGN TECHNOLOGY DIVISION

AIR FORCE SYSTEMS COMMAND

PRELIMINARY ANALYSIS OF RESULTS OF A MOUNTAIN AREA ATMOSPHERIC DIFFUSION TEST

FOREIGN TECHNOLOGY DIVISION

EDITED TRANSLATION

FTD-ID(RS)T-1637-83 8 December 1983

MICROFICHE NR: FTD-83-C-001496

PRELIMINARY ANALYSIS OF RESULTS OF A MOUNTAIN AREA ATMOSPHERIC DIFFUSION TEST

English pages: 24

Source: Unknown, pp. 26-35

Country of origin: China
Translated by: LEO KANNER ASSOCIATES
F33657-81-D-0264
Requester: DET 22
Approved for public release; distribution unlimited.

THIS TRANSLATION IS A RENDITION OF THE ORIGINAL FOREIGN TEXT WITHOUT ANY ANALYTICAL OR EDITORIAL COMMENT. STATEMENTS OR THEORIES ADVOCATED OR IMPLIED ARE THOSE OF THE SOURCE AND DO NOT NECESSARILY REFLECT THE POSITION OR OPINION OF THE FOREIGN TECHNOLOGY DIVISION.	PREPARED BY: TRANSLATION DIVISION FOREIGN TECHNOLOGY DIVISION WP.AFB, OHIO.

GRAPHICS DISCLAIMER

All figures, graphics, tables, equations, etc. merged into this translation were extracted from the best quality copy available.

PRELIMINARY ANALYSIS OF RESULTS OF A MOUNTAIN AREA ATMOSPHERIC DIFFUSION TEST

Atmospheric Testing Technical Group*

I. Preface

Following the continuous advances in industry, there has been an increasing amount of harmful gases discharged into the atmosphere each day. In order to guarantee that the atmospheric environment of human life satisfies air quality standards, it is necessary on the one hand to rationally lay out newly constructed enterprises and add controls to the discharge of substances by already constructed enterprises; on the other hand, it is necessary to announce in advance the future harm levels of pollutants. All of these items urgently demand an understanding of the diluting capabilities of the atmosphere towards pollutants under different meteorological conditions.

In recent years, because there have been an increasing number of factories built in varied mountain areas and along the coasts, research on low level atmospheric structures under non-uniform topographical conditions and atmospheric diffusion laws has been getting an increasing amount of serious attention. When comparing mountain areas and plains, the atmosphere near stratum structures and diffusion diluting capability are very different. The problems of how to fully use the beneficial factors of mountain areas, avoid non-advantageous conditions and reduce the industrial pollution of factories constructed in mountain areas so that the natural environment, the atmosphere, is the responsibility of engineering design and rational

*Composed of members of Qinghua University, Central Meteorological Department, Atmospheric Physics Institute of Chinese Academy of Sciences and Lanzhou Plateau Atmospheric Physics Institute. Beijing University, worker-peasant-soldier students of Qinghua University and the Geological Institute of the Chinese Academy of Sciences also participated in the work.

industrial layout is a major task of atmospheric physics workers.

This paper used the results of diffusion tests of artificial smoke clouds and neutron activated smoke in a certain mountain area during the spring and autumn of 1975 as well as related meteorological observation data. It also used different methods to calculate the atmospheric diffusion parameters of this mountain area especially focusing on the differences of the diffusion diluting capabilities of the pollutants in the mountain area and on the plain and compared them with related foreign results whereupon useful results were obtained.

II. General Situation of the Test and Sources of Data

1. Topography. The test site was a mountain area and its topography is as shown in Fig. 1. In the figure, point A is an iron tower with a height of 98.2 meters, the base of the tower is located on a platform 372 meters above sea level. To its west, north and east are high mountains and to the south it faces a level area. The tower is located on one end of a north-south running valley.

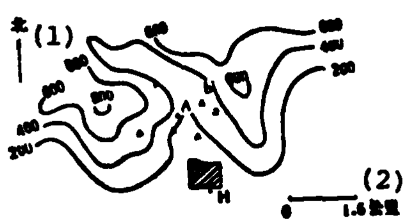

Fig. 1 Topography of the atmospheric test. The solid lines are contour lines (meters), A is the iron tower, ▲ is the photographing point, ab is the three-dimensional photographic datum line, ▨ is the architectural complex, H is the chimney.

Key: (1) North; (2) Kilometers.

2. Meteorological Observations on the Tower

The meteorological observation instruments were installed on the movable cantilever arm extending from the tower. The arm length is twice the length of the side of the tower. We used the electrical registering anemograph, thermister thermometer and hot line anemometer (separately at the eight heights of 2, 13.4, 22.4, 31.4, 44.9, 62.9, 80.9 and 97.4 meters) to measure the average wind and temperature gradients. Observations were done once an hour and the average time was 20 minutes. The horizontal wind direction pulsating data was obtained by an improved EL-2 instantaneous wind direction anemograph (installed at a height of 49.4 meters).

3. Artificial Smoke Cloud Diffusion Tests

48 kilogram smoke containers were erected at different heights on the iron tower and acted as release sources of the artificial smoke clouds. The amount of smoke produced by this method was uniform and the smoke issuing time of each container was 8-12 minutes. In the downwind direction of the flue we used the two methods of the common camera and the ground three-dimensional camera [1] to continuously photograph the smoke cloud. Each cloud could be continuously photographed 10 to 20 times and the sampling time was about 10 minutes.

4. Diffusion Tests of Tracer Elements

Twenty tests were carried out at heights of 80 meters on the iron tower. The emission of indium nitrate in each test was 200-500 grams and the emission mode was burning an alcohol solution of indium nitrate in a high pressure blowlamp to form indium oxide particles with diameters smaller than 0.1mm so as to simulate the diffusion movements of the discharged gases in the atmosphere. When released, they separately arranged fan-shaped specimen points on the seven arcs downwind 0.4, 0.8, 1.5, 3.0, 5.0, 10.0 and 45.0 kilometers (the relative elimination point tensor angle was 60°).

After completing the mountain tests, we also carried out 5 tests on level fields about 2 kilometers south of the tower. Seven specimen points were distributed equidistantly on four arcs (in a 60° fan-shape) downwind 50, 150, 250 and 450 meters. Each release was 100 grams of indium nitrate.

III. Use of the Photographic Method to Determine the Diffusion Parameters of the Smoke Cloud

1. Method for Calculating Diffusion Parameters

On the downwind side of the release point, we calculated the basic relationship of vertical diffusion parameter σ_x from the smoke cloud's average contour for the smoke cloud's locus photograph as [2]

$$\sigma_z^2 = z_c \left\{ \ln \frac{e z_m^2}{\sigma_z^2} \right\}^{-1} \qquad (1)$$

In the formula, z_c is the distance from the average flue axis to the visible boundary (also called the vertical half width), z_m is the maximum vertical half width and e is the bottom of the natural logarithm.

By using the graphic method to find transcendental equation (1), we can obtain vertical diffusion parameter σ_z based on the z_e measured on a certain downward distance. By using the completely analogous method, we can obtain diffusion parameter σ_y of the beam wind direction.

2. Major Results

Based on the various different conditions, we will now separately discuss the results obtained through observations as follows:

(1) Diffusion of Leeward Slope of Airflow Passed the Mountain

When there is a northwest wind passing the northern ridge, the smoke source's discharge point on the tower is located in the cavity area of the leeward slope and its diffusion characteristic point is the flue's inclined lower pressure and strong perturbation motion. See line 1 in Fig. 2a for the results of the average of the four data measured in the tests. (Afterwards, aside from special explanations, the stability is given based on Pasquill's [3] method of categorization.)

(2) Diffusion Under Local Circulation Control

a. Diffusion When the Wind is to the North

When there is no systematic airflow passed the mountain, there is a clear night and the main body of the cold air accumulated in the mountain area flows out from the eastern gorge. The wind direction of the smoke cloud's discharge point on the tower is predominantly northeastern and the flue is relatively stable. See solid line 2 in Fig. 2a for the mean results of the five data measured from tests.

b. Diffusion When the Wind is to the South

During 9 tests when there was wind towards the south the flue was even more stable than when there was a north wind because the airflow flowed from the level area to the mountain area and perturbation motion was relatively small. See lines 3 and 4 in Fig. 2a for the mean results.

(3) Diffusion of Opposite Level Area

In order to compare and discuss the differences of the diffusion of different positioned leeward slopes, we also photographed and measured the flue discharge from the chimney H (see Fig. 1) of the opposite level area. Its northern section was an architectural complex with a 500 square meter range and the average height was 20 meters. Its southern section was relatively level farmland and the chimney height was 37 meters.

When there was a systematic northwest wind and the chimney was still located in the wake flow area of the mountain area's rough air, adding on the influence of the architectual complex, the swinging of the flue was relatively large. See line 1 in Fig. 2b for the mean results of 4 measurements.

When the airflow blows from the south section's level area, the flue is relatively level and straight. See line 2 in Fig. 2b for the mean values of three measurements.

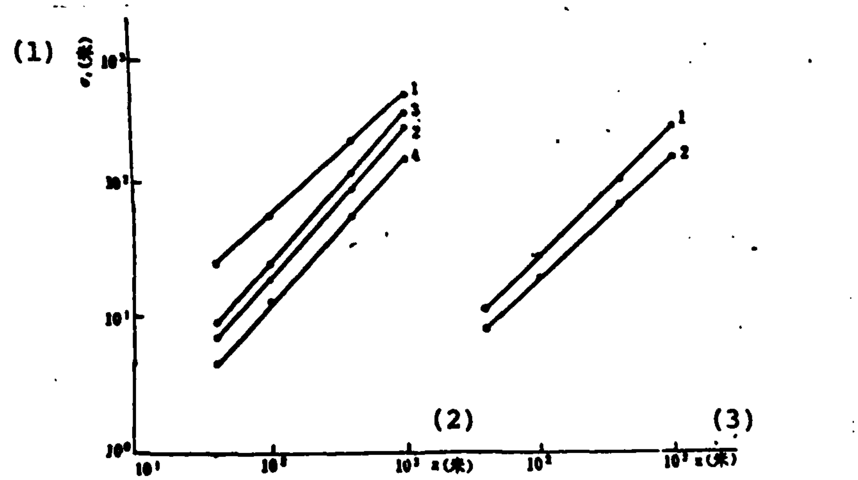

a. 山区情况，烟云释放高度为80米，平均时间10分钟

b. 平坦地形情况，烟囱高度37米，平均时间10分钟

Fig. 2 Curve of σ_z measured by photographic method changes with the distance.

(See next page for key)

Fig. 2 (continued)

Key: (a) Mountain area conditions are: smoke, cloud release height is 80 meters and mean time is 10 minutes; line 1 is strong northwestern wind, D type, average of 4 times; line 2 is northeastern wind, C-D type, average of 5 times; line 3 is the wind is to the south, type B, average of 5 times; line 4 is wind is to the south, type C, average of 4 times; O indicates the value of the measured point; (b) Level topographical conditions are: chimney height is 37 meters and mean time is 10 minutes; line 1 is northwestern wind, type C, average of 4 times; line 2 is wind is to the south, type B-C, average of 3 times; O indicates the value of the measured point; (1)-(3) Meters.

IV. Use of Wind Direction Pulsation Data to Calculate Diffusion Parameters

1. Calculation of Wind Direction Pulsation Standard Difference σ_θ

From statistical analysis of smoke cloud crosswise diffusion and release point wind direction pulsation data [4], we can obtain a method which uses the wind direction pulsation data to calculate the density distribution of the pollutants. Its wind direction pulsation standard difference is indicated as $(\sigma_\theta)_{\tau s}$. In this, τ is the sampling time, $s=\frac{x}{\beta\bar{u}}$ is the mean time, $\beta=\frac{T}{s}$ is the ratio of the Lagrangian time scale and the Eulerian time scale, $T=\frac{x}{u}$ is the particle movement time, x is the distance of the tailwind direction particle movement and $\bar{u}$ is the mean wind speed of the tailwind direction. Thus, $(\sigma_\theta)_{\tau,s}$ is the wind direction pulsation standard difference on the release point with the sampling time being τ and the mean time being $s=\frac{x}{\beta\bar{\bar{u}}}$. During tests, we used the improved EL-2 spontaneous anemorumbometer. Its inertial time is less than 5 seconds, the paper moving speed of the wind direction recorder is 0.5mm/second and in sampling time τ, it reads one wind direction pulsation θ_i' every 5 seconds. We obtained a new sequence of different θ_i' for the different mean times recorded as $\theta'_{s,i}$. Its variance is expressed as

$$\overline{\theta'^2_{\tau,s}} = (\sigma_\theta^2)_{\tau,s} = \frac{1}{N}\sum_{i=1}^{N}\left[\theta_{i,s} - \frac{1}{N}\sum_{i=1}^{N}\theta'_{i,s}\right]^2 \qquad (2)$$

In the formula, θ' is the horizontal wind direction pulsation value and N is the number of samples. From formula (2) we can derive the curve of $(\sigma_\theta)_{\tau,s}$ which changes with the mean time. We can also calculate the various σ_θ values with different degrees of stability.

2. Results of Calculation of β Values

By using the wind direction pulsation data on the tower (49.4 meters) and the diffusion test (smoke cloud and tracer element indium) data, we can establish the following relationship

$$\frac{\sigma_y^2}{x^2} = \overline{\theta'^2_{\tau,T/\beta}} \qquad (3)$$

When we determine the σ_y^3 of a certain distance x from the diffusion tests as well as the curve of observed $\overline{\theta'^2_{\tau,T/\beta}}$ which changes with s, we find and satisfy the s_o value of $\frac{\sigma_y^2}{x^2} = \theta'^2_{\tau,s_o}s_o$ on the curve. Then, from

$$\beta = x/\bar{u}s_0 \qquad (4)$$

we can find the β value. During the entire calculation, sampling time τ=10 minutes and $\bar{u}$ is the mean wind velocity within 10 minutes. For mountain area conditions, σ_y is obtained with x=1000 meters using the photographic method; for the level area, σ_y is obtained from the concentration distribution data of indium when x is within 450 meters. The calculation results of related β values are listed in Tables 1 and 2.

(1) 稳定度类	D-E						C-D		F	(2) 平均
β	2.4	2.4	2.9	1.7	1.6	1.4	2.1	1.5	2.0	2.0

Table 1 β values of mountain areas.
Key: (1) Stability type; (2) Mean.

(1) 稳定度类	D			B-C						(2) 平均
β	4.5	4.5	5.3	8.9	2.1	3.7	3.7	6.3	8.4	5.2

Table 2 β values of level area.
Key: (1) Stability type; (2) Mean.

We can see from the tables that in the opposite level area, β changes in the 2.1 to 8.9 range, the mean is 5.2 which is larger than the β value of 4 calculated by Hay and Pasquill [4] (distance source is 100 meters) and it is basically the same as the (distance source 400-800 meters) mean value of 5.4 (its changing range is 2.4-10.5) which we obtained in diffusion tests carried out at an open coastal mountain area. However, the value of β =2.0 for diverse mountain areas is lower than the above mentioned results. This shows that the strength of the mountain area's turbulent flow is larger than that of the level area and thus β tends to be small; on the other hand, the β determined by σ_y calculated from the photographed data still has a certain error and whether or not these results reflect the actual situation still awaits more accurate test data confirmation.

3. Relationship of σ_θ and the Sampling Time

The relationship of σ_θ and the sampling time can be empirically expressed as

$$\frac{\sigma_\theta(\tau_1)}{\sigma_\theta(\tau_2)} = \left(\frac{\tau_1}{\tau_2}\right)^p \qquad (5)$$

From the 6 two hour data observed on the tower in the mountain area, we separately calculated the 6 sets of $\sigma_\theta(\tau_i)$ of τ=10, 20, 30, 60, 90 and 120 minutes and afterwards using the linear regression analysis method very easily derived the p values. The mean of the p values of 6 data was 0.21 and its changing range is 0.14-0.31. The foreign plain areas [5] usually take p=0.2 which is the same as the results in this paper.

4. Results of Calculations of σ_y

Based on the obtained $(\sigma_\theta)_{\tau,s}$ and β values mentioned previously, we can very conveniently derive the σ_y values on different downwind distances. See Fig. 3 for the results of different wind directions and different stability types on mountain and level area topography.

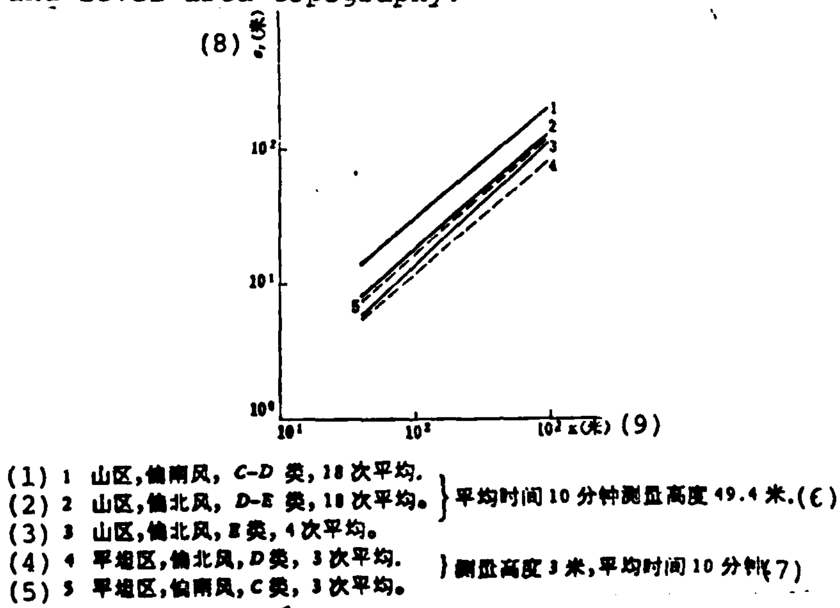

Fig. 3 Calculation of σ_y from wind direction pulsation data. (see next page for key)

Fig. 3 (continued)

Key: (1) Line 1, mountain area, wind to the south; C-D type, average of 18 times; (2) Line 2, mountain area, wind to the north, D-E type, average of 18 times; (3) Line 3, mountain area, wind to the north, E type, average of 4 times; (4) Line 4, level area, wind to the north, D type average of 3 times; (5) Line 5, level area, wind to the south, C type, average of 3 times; (6) Average time 10 minutes, measured height 49.4 meters; (7) Measured height 3 meters, mean time 10 minutes; (8) Meters; (9) Meters.

V. Use of Profile Data to Calculate Diffusion Parameters

1. Mean Wind Velocity Profile Characteristics

Based on the temperature vertical gradient, we divided the measured mean wind gradient data (145 times) into the three different stability types of tempera ture inversion, neutral and decreasing by degrees. See Fig. 4 for the mean wind velocity profile flow.

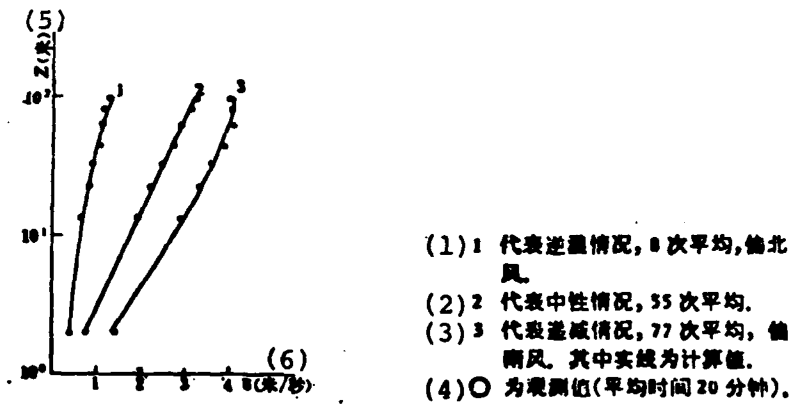

Fig. 4 Profiles of mountain area wind velocity.

Key: (1) Line 1 represents temperature inversion, average of 8 times, wind to the north; (2) Line 2 represents the neutral condition, average of 55 times; (3) Line 3 represents condition of decreasing by degrees, wind to the south. The solid line is the calculated value; (4) 0 is the measured value (mean time is 20 minutes); (5) Meters; (6) Meters/second.

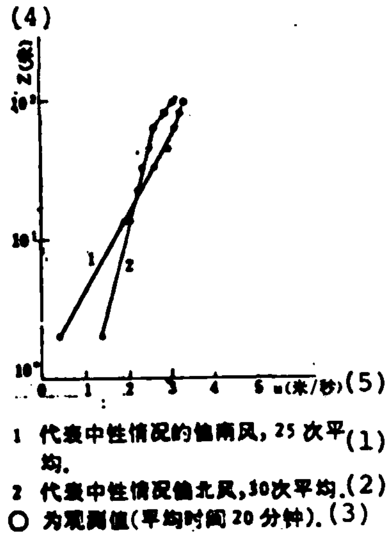

Fig. 5 Mean wind velocity profile under different wind direction conditions.

Key: (1) Line 1 represents the wind to the south in a neutral condition, average of 25 times; (2) Line 2 represents the wind to the north in a neutral condition, average of 30 times; (3) 0 is the measured value (mean time is 20 minutes); (4) Meters; (5) Meters/second.

We can see from profile 1 (average of 8 times) that up to a height of 100 meters, the mean wind velocity which follows the height distribution basically satisfies the logarithmic linear law's measured value and calculated value and the two are very similar. The wind direction is mainly to the north.

Profile 2 (average of 55 times) represents the mean wind velocity profile of the neutral layer junction. We can see that up to a height of 100 meters, the wind basically satisfies the logarithmic law and the calculated and measured values are the same. At the same time, it is easy to obtain the mean roughness length as 0.62 meters from the point of crossing of the straight line and longitudinal axis.

We can see from profile 3 (average of 77 times) that when below 60 meters, it can basically satisfy the logarithmic law and then the upwind velocity decreases very slowly with the height. However, the entire layer uses the logarithmic linear law for approximation and the calculated and measured values are quite similar. The wind direction is mainly to the south.

In order to explain the effects of surface roughness changes on the mean wind velocity profiles, we categorized the neutral layer junction data according to the wind direction. Curves 1 and 2 in Fig. 5 separately represent the mean wind velocity profiles of the wind to the south and to the north. We can see from this that the wind velocity profiles are all formed from two logarithmic profiles with different slopes. These two different slopes reflect the effects of the different roughness topographies on it. The low section shows the effect of the topography near the tower on the airflow and the high section shows noticeably different effects of more distant topography as compared with the roughness near the tower. Thus, the roughness lengths of the two sections are also different. There are also foreign results regarding the effects of topographical changes on the wind velocity profile. It is unanimously considered that there is an interface between the low layer effected by the topography near the tower and the high layer effected by more distant topography and that the profile on this interface shows points of inflection. The data analysis in this paper shows that the mean height of the points of inflection of the profiles is about 60 meters. The height of the single profile point of inflection varies with the difference of the wind direction.

2. Calculation of Logarithmic Linear Profile Parameters and Results

We can clearly see from the discussion in the above section that under non-neutral conditions, the mean wind velocity profiles can be approximated by the logarithmic linear relationship.

The meteorological observations carried out on the coast of Japan by Sensku [6] show that the height suitable for the logarithmic linear law can exceed 100 meters and can sometimes reach 200 meters. Aside from a small number of profiles which do not coincide with this law (for example, among 90 non-neutral profiles, there were 5 parabolic alphabets of lines under radiation temperature inversion conditions), this paper calculates the logarithmic linear profile parameters with various stability types.

The near ground layer similarity theory can only be applied when the stability and uniformity conditions are satisfied, but strictly speaking, the mountain areas in these tests were not satisfied. Here, we will use some relational formulas derived by the similarity theory as a type of empirical approximation but we will not carry out theoretical discussions. From the similarity theory of the near ground layer, we can express the average wind and temperature which follow the distribution of the height as [7]

$$\bar{u}(z) = \frac{u_*}{K}\left(\ln\frac{z}{z_0} + \alpha\frac{z}{L}\right) \quad (6)$$

$$T(z) - T(z_0) = T_*\left(\ln\frac{z}{z_0} + \alpha\frac{z}{L}\right) \quad (7)$$

In the formula, u_* is the friction speed, T_* is the temperature scale, K is the Karman constant (usually 0.4), z_0 is the roughness length, L is the Obukhov length scale and α is a universal constant.

In the same way, we assume that the average wind and temperature profiles of each observation can be written as the following experimental expressions

$$\bar{u}(z) = A_u \lg z + B_u z + C_u \quad (8)$$

$$T(z) = A_T \lg z + B_T z + C_T \quad (9)$$

In the formulas, A_u, B_u, A_T, B_T, C_u and C_T are the measured values of each wind and temperature profile derived by the binary linear regression method. Further through a contrastive analysis of formulas (6)-(9), we can derive the following relationships

$$\left.\begin{aligned} u_* &= 0.174\, A_u \ (\text{米/秒})^{(1)} & L &= 13.3 A_u^2/A_T \ (\text{米})^{(2)} \\ a &= 15.2\left(\frac{B_u}{A_u}+\frac{B_T}{A_T}\right)\frac{A_u^2}{A_T} & \lg z_0 &= -\frac{C_u}{A_u} \end{aligned}\right\} \qquad (10)$$

Key: (1) Meters/second; (2) Meters.

Based on the above method, we calculated a total of 42 profile examples in order to coordinate with the smoke cloud diffusion test data. There have already been many conclusions abroad related to the a values and for comparison the values of a are listed in Table 3.

作者 (1)	Deacon	Monin-Obukhov	Priestley	Yamamoto	Taylor	Panofsky	Kondo	Sensku	本文 (2)
a	2.25	0.6	4	2—12	2.5—12	4.5	3.3	1.07	1.8±1.15

Table 3 Table of comparison of a values [6].
Key: (1) Author; (2) This paper.

We can see from the table that aside from the values given by Monin-Obukhov and Sensku, the $a=1.8\pm1.15$ (0.5-4.6) value of this paper is the smallest. This is possibly related to the mountain area topography's perturbation motion being large which causes the wind velocity changes to become small.

3. Use of Profile Data to Calculate Diffusion Parameters

The vertical standard difference σ_x can be given by the following empirical relationship [8]:

$$\sigma_z = \frac{\sigma_w}{\bar{u}} g(x) \qquad (11)$$

In the formula, σ_w is the vertical wind velocity pulsation standard difference and g(x) is the distance function. From the results given by Monin [9], σ_w can be expressed as

$$\sigma_w \doteq u_* \left[1 - \frac{1}{f(\zeta)}\right]^{\frac{1}{2}} \qquad (12)$$

In the formula, $F(\zeta)$ is a universal constant and when calculating the bottom, all are approached using the logarithm linear relationship, $\zeta = \frac{z}{L}$. This equation is also derived under stable and uniform conditions. Here, we will only use this relational formula as a type of empirical approximation. Based on this processing, if there is a very large difference with the test results, this explains that this type of approximation is not rational; on the contrary, this type of approximation can be accepted in actual work and thus formula (12) can be written as

$$\left.\begin{aligned} L>0 \quad & \sigma_w = u_* \left[1 - \frac{\zeta}{1+\alpha\zeta}\right]^{\frac{1}{2}} \\ L<0 \quad & \sigma_w = u_* \left[1 + \frac{|\zeta|}{1-\alpha|\zeta|}\right]^{\frac{1}{2}} \end{aligned}\right\} \qquad (13)$$

In actual calculations, the g(x) in formula (11) is empirically given as x^r and r is given as $(r = \frac{2-n}{2})$ from the mean wind velocity based on the following formula of exponent n changing according to the exponential law

$$\bar{u} = \bar{u}_1 \left(\frac{z}{z_1}\right)^{\frac{n}{2-n}} \qquad (14)$$

Then

$$\left.\begin{array}{ll} L>0 & \sigma_z = \frac{u_*}{\bar{u}}\left[1-\frac{\zeta}{1+a\zeta}\right]^{\frac{1}{2}}\cdot x^{\frac{2-n}{2}} \\ L<0 & \sigma_z = \frac{u_*}{\bar{u}}\left[1+\frac{|\zeta|}{1-a|\zeta|}\right]^{\frac{1}{2}}\cdot x^{\frac{2-n}{2}} \end{array}\right\} \quad (15)$$

In the formulas, $\bar{u}$ takes the mean of the entire layer's wind velocity, u_*, a, L and $r=\frac{2-n}{2}$ are already calculated and given. z takes the geometric mean height of the observed layer (in the actual calculations, $z=\sqrt{97.4\times 2}\approx 14$ meters). Then, we can derive the relationship of σ_z which follows downwind distance x from the formula (15).

In order to test this method of calculating σ_z, we compared the calculated values and simultaneously test measured σ_z of the smoke cloud diffusion. From the test data on half thickness h of the smoke cloud's mean contour, by using the following approximation relationship

$$\sigma_z = \frac{h}{2.15} \quad (16)$$

we can very conveniently derive σ_z. Table 4 lists the data of 9 profile observations and as well as completely corresponding photography observations of the smoke cloud, (7 of which were the B-C type and 2 were the E type, including 4 day test data), and the results of 4 representative observations (including identical best and poorest examples).

(1) 时间 / σ_z (米) (2) / (3) 距离X (米)		40	60	80	100	150	200	300	稳定度类 (4)
5:30	(5) 烟实测	3.4	4.5	5.4	6.4	8.5	10.3	13.8	E
	(6) 计算	1.4	2.03	2.65	3.26	4.7	6.2	8.4	
8:36	(7) 烟实测	3.4	5.1	7.0	8.8	13.5	18.0	28.0	B-C
	(8) 计算	3.9	5.45	7.4	9.15	13.4	17.4	23.7	
9:20	(9) 烟实测	3.6	5.0	6.4	7.8	11.0	14.0	20.0	B-C
	(10) 计算	3.04	4.4	5.75	7.05	10.2	13.4	18.2	
10:30	(11) 烟实测	3.6	5.1	6.6	8.1	11.5	15.0	21.5	B-C
	(12) 计算	2.8	3.94	5.1	6.2	8.9	11.5	16.4	

Table 4 Comparison of calculation of σ_z and measurement of smoke cloud.

Key: (1) Time; (2) Meters; (3) Distance X (meters); (4) Stability type; (5) Measurement of smoke; (6) Calculated; (7) Measurement of smoke; (8) Calculated; (9) Measurement of smoke; (10) Calculated; (11) Measurement of smoke; (12) Calculated.

We can see from Table 4 that by using the similarity theory method, from the mean wind and temperature profile data, the derived vertical diffusion parameters and actual situation have relatively good uniformity. The uniformity is even better under unstable conditions. In order to further explain the level of uniformity of the calculated and measured values, we did statistics on the ratio of the calculated and measured values of σ_z of the 9 examples (40-300 meters). Results showed that 76.1% had the ratio smaller than 1.5, 87.2% had the ratio smaller than 2 and those with ratios larger than 2 were examples of the E type. This explains that even though the uniform conditions of the mountain area are difficult to satisfy, when the similarity theory method is used empirically, it cannot cause relatively large errors. We applied this method and calculated a total of 42 examples and divided them into 5 stability types based on length, dimension and size. Each mean parameter is listed in Table 5. See Fig. 6 for results of calculations of σ_z.

(1) 稳定度类	(2) L(米)	(3) Pasquill 稳定度类[3]	(4) 次数	(5) u_* (米/秒)	α	(6) ū (米/秒)	r
I	−27	B-C	14	0.290	1.8	2.70	0.98
II	−100	C-D	9	0.442	1.8	3.94	0.96
III	−300	D-E	6	0.280	1.8	2.80	0.94
V	100	E-F	8	0.133	1.8	1.90	0.91
VI	25	F	5	0.086	1.8	1.30	0.87

Table 5 Table of calculations of parameters of σ_z.
Key: (1) Stability type; (2) Meters; (3) Stability type; (4) Number of times; (5) Meters/second; (6) Meters/second.

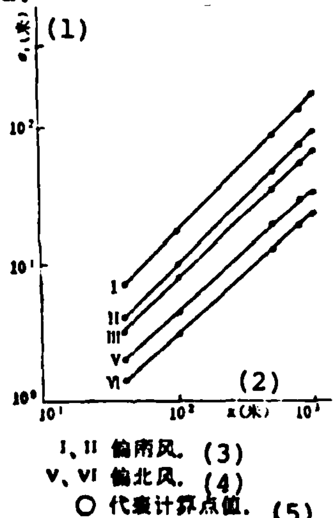

Fig. 6 Diffusion parameter σ_z calculated by profile data.
Key: (1) Meters; (2) Meters; (3) I and II, wind to south; (4) V and VI, wind to the north; (5) O represents calculated point value.

VI. Use of Concentration Distribution of Indium to Calculate Diffusion Parameters

We used the measured indium ground concentration data to separately calculate the horizontal and vertical diffusion parameters. The σ_z is given by

$$\sigma_y^2 = \frac{\Sigma C_i y_i^2}{\Sigma C_i} - \left(\frac{\Sigma C_i y_i}{\Sigma C_i}\right)^2 \qquad (17)$$

In the formula, C_i is the sampling point's measured concentration. σ_z is derived by the corsswire integral concentration method. Its expression is

$$C_c = \int_{-\infty}^{\infty} C dy = \sum_{i=1}^{N} C_i \Delta y = \sqrt{\frac{2}{\pi}} \frac{Q}{\sigma_z \bar{u}} e^{-\frac{H^2}{2\sigma_z^2}} \qquad (18)$$

In the formula, when crosswire integral concentration C_c, source strength Q, mean wind velocity $\bar{u}$ amd effective source height H are all known quantities, we can then derive σ_z.

By using the above processing method, we calculated the test data of 3 level topographical conditions with the wind to the south. See Fig. 7 for results of σ_z and σ_y.

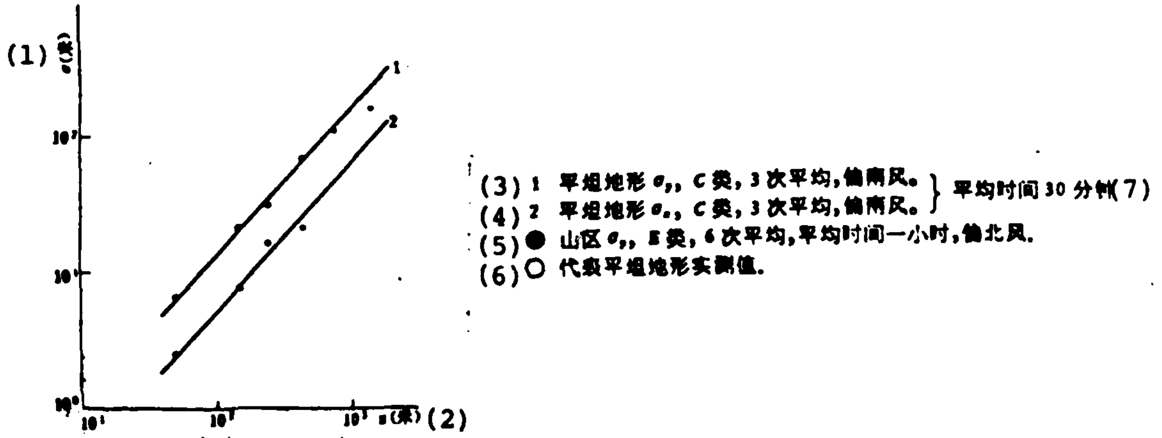

Fig. 7 Diffusion parameters calculated from concentration distribution of indium.

(see next page for key)

Fig. 7 (continued)

Key: (1) Meters; (2) Meters; (3) Line 1, level topography σ_y, C type, average of 3 times, wind to the south; (4) Line 2, level topography σ_z, C type, average of 3 times, wind to the south; (5) ● is mountain area σ_y, E type, average of 6 times, average time of one hour, wind to the north; (6) O represents measured value of level topography; (7) Average time of 30 minutes.

For the 20 tests on the mountain areas, because the topographical fluctuations within 800 meters were very large, the concentration did not satisfy the normal distribution. Beginning from 800 meters, the topographical fluctuations were relatively small and their concentrations approached satisfying the normal distribution. We only calculated 9 E type (wind to the north) weather examples of σ_y on 800 and 1500 meter arcs. See Fig. 7 for mean results.

VII. Discussion of Results

1. Comparison of Mountain Area and Plain Diffusion Parameters

The diffusion parameters of mountain area parameters are usually larger than those of the plain because of topographical fluctuations. For comparison, we compared Pasquill-Gifford's [5] representative values of σ_y and σ_z as the plain conditions interpolated from the curve of the diffusion parameters which change with the distance and the results of the same stabilities given by the four methods of this paper. The ratios of the 800 meter area diffusion parameters are listed in Table 6.

(1) 天气类型 / (2) 比值 / (3) 方法	(8) C(南风) σ_y/σ_{yP}	σ_z/σ_{zP}	(9) E(北风) σ_y/σ_y	σ_z/σ_{zP}
(4) 铟	$1.3_{平}$ (11)	$0.9_{平}$ (15)	$2.4_{山}$ (18)	—
(5) 廓线法	—	$1.9_{山}$ (16)	—	$2.2_{山}$ (20)
(6) 照相法	$2.5_{山}$ (12)	$2.5_{山}$ (17)	—	—
(7) 脉动法	$2.5_{山}$ (13) $1.1_{平}$ (14)	— —	$2.0_{山}$ (19) —	— —

(10)* 凡标有P的表示 Pasquill 平原情况的值,下标有"平"的表示平坦地形观测结果,下标有"山"的表示山区结果

Table 6 Ratio of mountain area and plain diffusion parameters*.

Key: (1) Type of weather; (2) Ratio; (3) Method; (4) Indium; (5) Profile method; (6) Photographic method; (7) Pulsation method; (8) South wind; (9) North wind; (10)* The ordinary notation of P indicates the value of the Pasquill plain condition, the lower notation of "level" indicates the observation result of level topography and the lower notation of "mountain" indicates the observation results of mountain areas; (11) Level; (12) Mountain; (13) Mountain; (14) Level; (15) Level; (16) Mountain; (17) Mountain: (18) Mountain; (19) Mountain; (20) Mountain.

We can see that the indium made from the level area and the σ_y and σ_z calculated from the wind direction pulsation data are basically the same as the Pasquill results with the same stability type. When comparing the same type of weather of the mountain area and Pasquill, the mountain area σ_z is 1.9-2.5 times that of the plain and the mountain area σ_y is 2.0-2.5 times that of the plain. Therefore, we can generally consider that the diffusion parameters of the mountain area are 2.0-2.5 times those of the plain's diffusion parameters. When the wind is especially strong, the topographical perturbation is even stronger. If we use the photographic method, when there is a strong northwest wind of the D type, mountain area σ_z is 8 times that of the plain. Therefore, from these test results which are average conditions, we can approximately consider that if we use the diffusion parameters of plain conditions to estimate the concentrations of mountain areas, then it is 4-6 times the actual height. Houind [10] carried out plateau diffusion tests in certain mountain lands of a mountain area and the results of D type weather $C_{calculated}/C_{measured}=$ 6.0 are identical to those of this paper. In the same way, Start [11] carried out separate diffusion tests on the tops of mountains and in mountain valleys and the neutral condition (equivalent to the C-D type) $C_{calculated}/C_{measured}=5$ also is basically the same as the results in this paper.

2. Relationship of Mountain Area's Diffusion Parameters and Wind Direction

Because of the non-uniformity of the mountain area topography's roughness space distribution, great differences are created in the diffusion parameters which follow the direction of the airflow. If the wind is to the south, the topography is relatively level and when the wind is to the north, the upstream is the topography of the high mountain fluctuations. These two conditions have very large differences towards the perturbation of the airflow. By comparing lines 1 and 2 and 3 and 4 of Fig. 2a, we can see that the C-D type of the northeast wind is close to twice as large as the C type σ_z of the south wind and when there is a strong northwest wind, it is even larger. If there is a strong northwest wind, the σ_z of the D type is also much larger than the B type when there is a south wind. Given the same stability type, it can reach 4-5 times larger. Therefore, the wind direction is a very important factor in selecting the mountain area's diffusion parameter.

3. The Mean Wind Velocity Profile Characteristics of the Mountain Area's Near Ground Layer

The mountain area's mean wind gradient data of the near ground layer less than 100 meters shows that when there are non-neutral conditions, the mean wind velocity profile can be approximated by the logarithmic linear law. Its α value is much smaller than that of the plateau and the mean results of this paper is 1.8± 1.15. The vertical direction perturbation of this topography is large which creates mixed uniformity. Neutral conditions basically satisfy the logarithmic distribution and the roughness length is 0.62 meters.

References

[1] Glacial Soil Desert Institute of the Chinese Academy of Sciences, Measurement Basis of Ground Three-Dimensional Photography and Its Applications, 1973.

[2] U.S. Atomic Energy Commission, Meteorology and Atomic Energy, 1968.

[3] H.E. Hesketh, Understanding & Controlling Air Pollution,1972.

[4] J.S. Hay and F.Pasquill, Advances in Geophysics,1959,6, p471.

[5] D.B. Turner, PB 191482, 1970.

[6] T. Sensku, Symposium On Atmospheric Diffusion and Air Pollution, 1974, PP180-183.

[7] K.Takeuchi, J.Meteor.,Soc. Japan,1961, 39(6) PP 346-367.

[8] H.A. Panofshy and B. Prasad, Int.J. Air. Wat. Poll. 1965, 9(7-8), P419.

[9] A.S. Monin, the same as [4], PP331-341.

[10] E. Houind, the same as [6], PP214-217.

[11] G.E. Start, the same as [6], PP226-232.

FTD-ID(RS)T-1632-83

一次山区大气扩散试验结果的初步分析

大气试验技术小组*

一、前　言

随着工业的不断发展，每天排放到大气中的有害气体越来越多，要保证人们生活的大气环境满足空气质量标准，一方面对新建企业要作合理布局，对已建企业的排放物质要加以控制；另一方面对污染物质未来的危害程度要作预告．所有这些，都迫切要求了解不同气象条件下大气对污染物质的稀释能力．

近年来，由于在复杂山区和海岸沿线的建厂越来越多，因而不均匀地形条件下低层大气结构和大气扩散规律的研究也日益受到重视．山区与平原相比，大气近地层结构和扩散稀释能力都很不相同．如何充分利用山区的有利因素，避开不利条件减少山区建厂的工业污染，使大气这个自然环境为工程设计和工业合理布局服务是大气物理工作者的一项重要任务．

本文利用 1975 年春秋两季，在某山区作的人工烟云和中子活化铟的扩散试验结果及有关的气象观测资料，用不同方法计算了该地区的大气扩散参数，特别强调了污染物在山区和平原扩散稀释能力的差别，并和国外有关结果进行比较，得出一些有益的结果．

二、实验概况及资料来源

1. 地形　实验地点为一山区，其地形如图 1 所示．图中 A 点为高 98.2 米的铁塔，塔基位于海拔 372 米的台地上．它的西、北和东面为高山地形，南面为相对平坦区．塔处在南北走向山沟出口处的一侧．

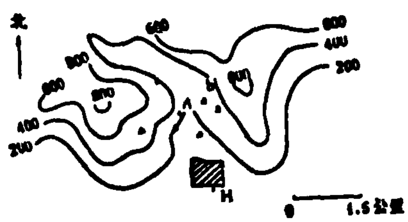

图 1　大气试验地形　实线为等高线（米），A 为铁塔 ▲摄影点，ab为立体摄影基线 ▨建筑群，H 为烟囱

2. 塔上的气象观测　气象观测仪器安装在从塔架伸出来的活动悬臂上，臂长为塔身边长的 2 倍．应用电接风向风速计、热敏电阻温度计和热线风速仪（分别在 2、13.4、22.4、31.4、44.9、62.9、80.9 和 97.4 米八个高度上）作平均风和温度梯度测．每小时观测一次，平均时间为20分钟．水平风向脉动资料，采用改进后的 EL-2 型瞬时风向风速计（安装在 49.4 米高度上）获得．

* 由清华大学、中央气象局、北京大学、中国科学院大气物理研究所和兰州高原大气物理研究所派员组成．参加工作的还有北京大学、清华大学工农兵学员和中国科学院地理研究所．

3. 人工烟云扩散试验　在铁塔不同高度上架设 48 公斤重的烟罐，作为人工烟云的释放源．这种方法产生的烟量均匀，每罐发烟时间为 8—12 分钟．在烟道的下风方，用普通相机和地面立体摄影机[1] 两种方法对烟云进行连续拍照，每次烟云可连续拍摄十至二十张照片，取样时间约 10 分钟．

4. 示踪元素铟的扩散试验　在铁塔 80 米高度上进行了 20 次试验，每次硝酸铟的发射量为 200—500 克，其发射方式是将硝酸铟的酒精溶液在高压喷灯里燃烧，形成直径小于 0.1 微米的氧化铟微粒，以模拟排放气体在大气中的扩散运行情况．释放时分别在下风方向 0.4、0.8、1.5、3.0、5.0、10.0 及 45.0 公里的七道弧上（相对排放点张角为60°）的扇形布置采样点．

在完成山地试验后，还在塔的南边约 2 公里的平坦田野进行了五次试验．分别在下风方 50、150、250 和 450 米的四道弧上（60° 扇形内）等距地布七个采样点．每次释放硝酸铟量为 100 克．

三、用照相方法测定烟云的扩散参数

1. 扩散参数的计算方法　在释放点的下风侧，对烟云轨迹拍照，由烟云平均轮廓计算垂直扩散参数 σ_z 的基本关系为[2]

$$\sigma_z^2 = z_e \left\{ \ln \frac{e z_m^2}{\sigma_z^2} \right\}^{-1} \tag{1}$$

式中 z_e 为平均烟道轴线到可见边缘的距离（或称垂直半宽度）z_m 为最大垂直半宽度，e 为自然对数的底．

应用图解法求解超越方程（1），就可根据在下风方某一距离上量测的 z_e 和 z_m 值得到垂直扩散参数 σ_z．用完全类似的方法，可以得到横风方向的扩散参数 σ_y．

2. 主要结果　按照各种不同条件，现将观测得到的结果分述如下：

（1）过山气流背风坡的扩散　当有西北风越过北部山脊时，塔上烟源排放点恰好位于背风坡的空腔区内，其扩散特点是烟道倾斜下压和强烈的扰动，试验测得的四次资料平均结果见图 2a 直线 1．（以后除特殊说明外，稳定度均按 Pasquill[3] 分类方法给出．）

（2）地方性局地环流控制下的扩散

a. 偏北风情况的扩散　当没有系统过山气流时，晴天夜间，山区堆积的冷空气主体由东部峡谷中流出．塔上烟云施放点的风向以东北风为主，烟道比较平稳，试验测得的五次资料平均结果见图 2a 直线 2．

b. 偏南风情况的扩散　在偏南风条件下的 9 次试验中，由于气流从平坦区流向山区，扰动较小，烟道比偏北风时更平稳，其平均结果见图 2a 直线 3 和 4．

（3）相对平坦区的扩散　为了比较说明背风坡不同位置扩散状况的差别，对相对平坦区的烟囱 H（见图 1）排放出来的烟道，也进行了拍摄和量测．它的北部为 500 平方米范围的建筑群，平均高度为 20 米，它的南部是比较平坦的农田，烟囱高度为 37 米．

当有系统西北风时，烟囱仍处于高山扰流的尾流区中，加上建筑群的影响，烟道摆动仍较大，4 次量测的平均结果见图 2b 直线 1．

当气流从南部平坦地区吹来时，烟道比较平直，三次量测的平均值见图 2b 直线 2．

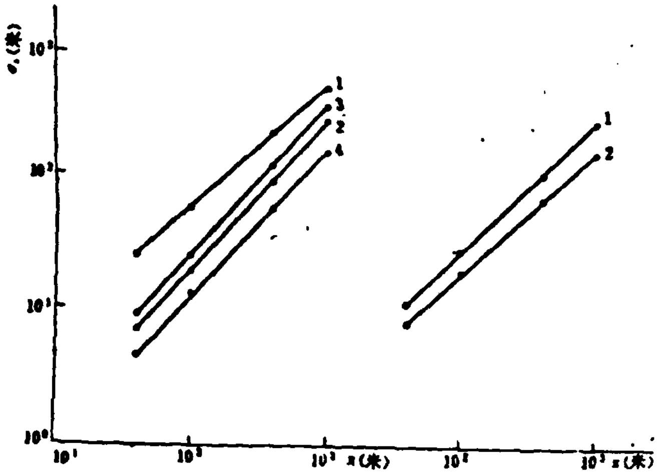

a. 山区情况，烟云释放高度为 80 米，平均时间 10 分钟

1 西北大风，D 类，4 次平均.
2 东北风，C–D 类，5 次平均.
3 偏南风，B 类，5 次平均.
4 偏南风，C 类，4 次平均.
0 表示量测点值

b. 平坦地形情况，烟囱高度 37 米，平均时间 10 分钟

1 西北风，C 类，4 次平均.
2 偏南风，B–C 类，3 次平均.
0 表示测量点值.

图2 照相法测得的 σ_y 随距离变化曲线

四、用风向脉动资料计算扩散参数

1. 风向脉动标准差 σ_θ 的计算 由烟云横向扩散和释放点风向脉动资料的统计分析[4]，可得出风向脉动资料推算污染物浓度分布的方法. 其风向脉动标准差表示成 $(\sigma_\theta)_{\tau,s}$，其中 τ 为取样时间，$s=\frac{x}{\beta\bar{u}}$ 为平均时间，$\beta=\frac{T}{s}$ 为拉格朗日时间尺度和欧拉时间尺度之比，$T=\frac{x}{\bar{u}}$ 为质点运行时间，x 为顺风方向质点行走的距离，$\bar{u}$ 为顺风方向的平均风速. 因而，$(\sigma_\theta)_{\tau,s}$ 是在释放点上，取样时间为 τ，平均时间为 $s=\frac{x}{\beta\bar{u}}$ 的风向脉动标准差. 在实验中，采用改进后的 EL-2 型瞬时风向风速计，其惯性时间小于 5 秒，风向记录器的走纸速度为0.5毫米/秒，在取样时间 τ 内，每 5 秒读一个风向脉动值 θ'_i，对不同的平均时间，得到不同的 θ'_i 的新序列，记为 $\theta'_{i,s}$，其方差表达成

$$\overline{\theta'^2_{\tau,s}}=(\sigma_\theta^2)_{\tau,s}=\frac{1}{N}\sum_{i=1}^{N}\left[\theta'_{i,s}-\frac{1}{N}\sum_{i=1}^{N}\theta'_{i,s}\right]^2 \tag{2}$$

其中 θ' 为水平风向脉动值，N 为样品数. 由 (2) 可以导出 $(\sigma_\theta)_{\tau,s}$ 随平均时间 s 的变化曲线，也可计算出各种不同稳定度类的 σ_θ 值.

2. β 值的计算结果 利用塔上（49.4 米）风向脉动资料及扩散试验（烟云和示踪元素铟）资料，可以建立以下关系

$$\frac{\sigma_y^2}{x^2}=\overline{\theta'^2_{\tau,T/\beta}} \tag{3}$$

由扩散实验测定某一距离 x 处的 σ_y^2，与同时观测的 $\overline{\theta'^2_{\tau,T/\beta}}$ 随 s 变化的曲线，在曲线上找出满足 $\frac{\sigma_y^2}{x^2}=\overline{\theta'^2_{\tau,s_0}}$ 的 s_0 值．则由

$$\beta = x/\bar{u}s_0 \tag{4}$$

可以求出 β 值．在整个计算中，取样时间 $\tau=10$ 分钟，$\bar{u}$ 为10分钟内的平均风速，对山区情况，σ_y 是用照相法在 $x=1000$ 米以内得到的；对平坦区，σ_y 是由氯的浓度分布资料，x 在 450 米以内得到的．有关 β 值的计算结果列于表 1 和表 2．

表 1　山区 β 值

稳定度类	D-E	C-D	E	平　均
β	2.4　2.4　2.9　1.7　1.6　1.4	2.1　1.5	2.0	2.0

表 2　平坦区 β 值

稳定度类	D	B-C	平　均
β	4.5　4.5　5.3	8.9　2.1　3.7　3.7　6.3　8.4	5.2

从表中看出，在相对平坦地形区，β 在 2.1 到 8.9 范围内变化，平均为 5.2，比 Hay 和 Pasquill[4] 计算的（距源 100 米处）β 值 4 偏大，与我们在某海岸开阔山地做的扩散试验得到的（距源 400—800 米）平均值 5.4（其变化范围为 2.4—10.5）基本一致．而复杂山区 $\bar{\beta}=2.0$，这个值比上述结果偏低，这一方面反映了山区湍流强度比平坦区大，因而 β 偏小；另一方面，由照相资料测得的 σ_y 所决定的 β 还存在一定误差，本结果是否反映实际情况，还有待更多更准确的实验资料证实．

3. σ_θ 与取样时间的关系　　σ_θ 与取样时间 τ 的关系可以经验地表示为

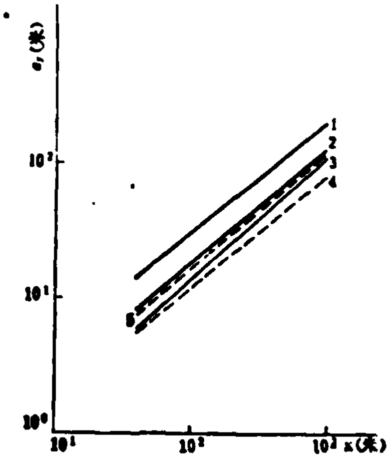

1　山区，偏南风，C-D 类，18 次平均．
2　山区，偏北风，D-E 类，18 次平均．} 平均时间 10 分钟测量高度 49.4 米．
3　山区，偏北风，E 类，4 次平均．
4　平坦区，偏北风，D 类，3 次平均．} 测量高度 3 米，平均时间 10 分钟．
5　平坦区，偏南风，C 类，3 次平均．

图 3　由风向脉动资料计算 σ_y

$$\frac{\sigma_\theta(\tau_1)}{\sigma_\theta(\tau_2)} = \left(\frac{\tau_1}{\tau_2}\right)^p \tag{5}$$

从 6 次山区塔上观测的 2 小时资料中，分别计算了 $\tau = 10$、20、30、60、90 和 120 分钟的 6 组 $\sigma_\theta(\tau_i)$，然后应用线性回归分析方法，很容易求出 p 值来. 6 次资料 p 值平均为 0.21，其变化范围为 0.14—0.31，国外平原地区[5]通常取 $p = 0.2$，与本文结果较为一致.

4. σ_y 的计算结果　根据前面已经得到的 $(\sigma_\theta)_{t,i}$ 和 p 值，可以很方便地求出不同下风方距离上的 σ_y 值，对山区和平坦地形不同风向和不同稳定度类的结果见图 3.

五、用廓线资料计算扩散参数

1. 平均风速廓线特征　我们将所观测的平均风梯度资料（145 次），按照温度垂直梯度分成逆温、中性和递减三种不同稳定度类型，每类的平均风速廓流见图 4.

从廓线 1（8 次平均）看出，直到 100 米高度，平均风速随高度分布基本上满足对数线性规律观测值和计算值两者相当一致. 其风向主要为偏北风.

廓线 2（55 次平均）代表中性层结的平均风速廓线. 可以看出，直到 100 米高度，风基本上满足对数规律，计算值与观测值一致. 同时，很容易由直线与纵轴交叉点得到平均粗糙度长度为 0.62 米.

从廓线 3（77 次平均）看出，60 米以下基本上满足对数规律，再往上风速随高度很慢地减小. 不过，整层用对数线性规律去逼近，计算值与观测值比较一致. 其风向主要为偏南风.

为了说明地面粗糙度变化对平均风速廓线的影响，我们将中性层结资料又按风向进行了分类，图 5 的曲线 1 和 2 就是分别代表偏南风和偏北风的平均风速廓线. 从中看出，风速廓线均由两根不同斜率的对数廓线组成，这两种不同斜率反映了两种不同粗糙度地

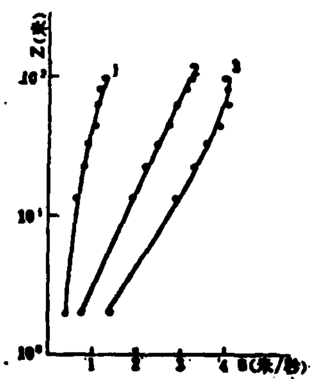

1　代表逆温情况，8 次平均，偏北风.
2　代表中性情况，55 次平均.
3　代表递减情况，77 次平均，偏南风. 其中实线为计算值.
○　为观测值（平均时间 20 分钟）.

图 4　山区平均风速廓线

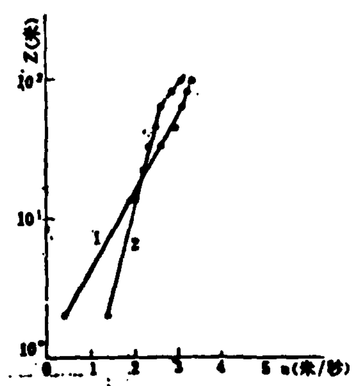

1　代表中性情况的偏南风，25 次平均.
2　代表中性情况偏北风，30次平均.
○　为观测值（平均时间 20 分钟）.

图 5　不同风向条件下的平均风速廓线

形对它的影响，低的部份表示塔附近地形对气流的影响，高的部份反映了与塔附近粗糙度明显不同的更远地形影响，因而两部分的粗糙度长也不一样．关于地形变化对风速廓线的影响国外已有一些结果，比较一致地认为受塔附近地形影响的低层与受更远的地形影响的高层气流之间有个界面，在这个界面上廓线出现拐点．本文资料分析表明，廓线拐点高度平均在60米左右，对单个廓线拐点高度随风向不同而异．

2. 对数线性廓线参数计算及结果　　从上一节讨论清楚看出，在非中性情况下，平均风速廓线均可用对数线性关系去逼近．Senshu[6] 在日本沿岸的气象观测表明，对数线性规律适用高度可超过100米，有时可达200米．除了少数不符合此规律的廓线（如90次非中性廓线中有5次辐射逆温条件下的抛物线型）外，本文作了各种稳定度类的对数线性廓线参数的计算．

近地面层相似理论只有在平稳均匀条件满足时才能应用，而本实验地处山区，严格讲是不满足的．我们这里借用一些由相似理论导出的关系式，作为一种经验性的近似，不作理论讨论．由近地面层的相似理论，平均风和温度随高度分布可以表达成[7]

$$\bar{u}(z)=\frac{u_*}{K}\left(\ln\frac{z}{z_0}+\alpha\frac{z}{L}\right) \tag{6}$$

$$T(z)-T(z_0)=T_*\left(\ln\frac{z}{z_0}+\alpha\frac{z}{L}\right) \tag{7}$$

式中 u_* 是摩擦速度，T_* 是温度尺度，K 为卡门常数（通常为0.4），z_0 为粗糙度长，L 为 Obukhov 长度尺度，α 为一普适常数．

同样，我们假设每次观测的平均风和温度廓线，可以写成以下实验表达式

$$\bar{u}(z)=A_u\lg z+B_u z+C_u \tag{8}$$

$$T(z)=A_T\lg z+B_T z+C_T \tag{9}$$

式中 A_u、B_u、A_T、B_T、C_u 和 C_T 由每次风和温度廓线的实测值，应用二元线性回归方法求出．又由(6)—(9)对比分析，可以导出以下关系

$$\left.\begin{aligned} &u_*=0.174A_u\ (\text{米/秒}) \qquad &L=13.3A_u^2/A_T\ (\text{米})\\ &\alpha=15.2\left(\frac{B_u}{A_u}+\frac{B_T}{A_T}\right)\frac{A_u^2}{A_T} \qquad &\lg z_0\doteq-\frac{C_u}{A_u}\end{aligned}\right\} \tag{10}$$

按照上述方法，为配合烟云扩散试验资料，一共计算了42次廓线例子．有关 α 值国外已有很多结果，为了比较将有关 α 的值列于表3．

表3　α 值比较表[6]

作者	Deaco	Monin-Obukhov	Priestley	Yamamoto	Taylor	Panofsky	Kondo	Sensku	本　文
α	2.25	0.6	4	2—12	2.5—12	4.5	3.3	1.07	1.8±1.15

从表看出，除了 Monin-Obukhov 和 Sensku 给出的值外，本文的 $\alpha=1.8\pm1.15$（0.5—4.6）值最小，这可能与山区地形扰动大，使风速变动变小有关．

3. 用廓线资料计算扩散参数　　垂直方向标准差 σ_z 可用以下经验关系[8]

$$\sigma_z=\frac{\sigma_w}{\bar{u}}g(x) \tag{11}$$

给出，式中 σ_w 为垂直方向风速脉动标准差，$g(x)$ 为距离函数．由 Monin[9] 给出的结果，

σ_w 可表达成

$$\sigma_w \doteq u_* \left[1 - \frac{1}{f'(\zeta)}\right]^{\frac{1}{4}} \tag{12}$$

式中 $f(\zeta)$ 为一普适函数，下面计算时，均用对数线性关系逼近，$\zeta = \frac{z}{L}$. 此方程也是在平稳均匀条件下导出来的，我们这里借用这个关系式，只作为一种试验性的近似。按此处理，如果与实验结果的相差很大，说明这种近似并不合理；反之，这样的近似实际工作中是可以接受的．则（12）式可写成．

$$\left.\begin{aligned} L > 0 \qquad \sigma_w &= u_* \left[1 - \frac{\zeta}{1 + \alpha\zeta}\right]^{\frac{1}{4}} \\ L < 0 \qquad \sigma_w &= u_* \left[1 + \frac{|\zeta|}{1 - \alpha|\zeta|}\right]^{\frac{1}{4}} \end{aligned}\right\} \tag{13}$$

（11）式中的 $g(x)$，在实际计算中，经验地给成 x^r，r 由平均风速按下式指数规律变化的指数 n 给出 $\left(r = \frac{2-n}{2}\right)$.

$$\bar{u} = \bar{u}_1 \left(\frac{z}{z_1}\right)^{\frac{n}{2-n}} \tag{14}$$

则

$$\left.\begin{aligned} L > 0 \qquad \sigma_z &= \frac{u_*}{\bar{u}1} \left[1 - \frac{\zeta}{1 + \alpha\zeta}\right]^{\frac{1}{4}} \cdot x^{\frac{2-n}{2}} \\ L < 0 \qquad \sigma_z &= \frac{u_*}{\bar{u}} \left[1 + \frac{|\zeta|}{1 - \alpha|\zeta|}\right]^{\frac{1}{4}} \cdot x^{\frac{2-n}{2}} \end{aligned}\right\} \tag{15}$$

式中 $\bar{u}$ 取整层风速的平均，u_*、α、L 及 $r = \frac{2-n}{2}$ 已经计算给出．z 取观测层的几何平均高度，（在实际计算中，$z = \sqrt{97.4 \times 2} \approx 14$ 米）．则由（15）式可导出 σ_z 随下风方距离 x 的关系来．

为了对这种计算 σ_z 的方法作检验，我们将计算值和同时作的烟云扩散实验实测的 σ_z 进行比较．由烟云平均轮廓的半厚度 h 的实测资料，应用以下的近似关系

表 4　计算 σ_z 和烟云实测比较

时间	σ_z（米） \ 距离X（米）	40	60	80	100	150	200	300	稳定度类
5:30	烟实测	3.4	4.5	5.4	6.4	8.5	10.3	13.8	E
	计　算	1.4	2.03	2.65	3.26	4.7	6.2	8.4	
8:36	烟实测	3.4	5.1	7.0	8.8	13.5	18.0	28.0	B-C
	计　算	3.9	5.45	7.4	9.15	13.4	17.4	23.7	
9:20	烟实测	3.6	5.0	6.4	7.8	11.0	14.0	20.0	B-C
	计　算	3.04	4.4	5.75	7.05	10.2	13.4	18.2	
18:30	烟实测	3.6	5.1	6.6	8.1	11.5	15.0	21.5	B-C
	计　算	2.8	3.94	5.1	6.2	8.9	11.5	16.4	

$$\sigma_z = \frac{h}{2.15} \tag{16}$$

可以很方便地求出 σ_z 来. 由 9 次廓线观测和烟云照相时间完全对应的资料(其中七次属 B-C 类两次属 E 类, 包括四天实验资料), 两种方法计算的 4 次有代表性(包括一致性最好和最差的例子)的结果列于表 4.

从表 4 可以看出,应用相似理论方法, 由平均风和温度廓线资料, 导出的垂直扩散参数与实际情况有较好的一致性, 尤其在不稳定条件下一致性更好. 为了进一步说明计算值与实测值一致的程度, 我们将这九次例子(40—300 米之间)所有 σ_z 的计算值与实测值的比值作了统计, 结果表明: 比值小于 1.5 的占 76.1%, 小于 2 的占 87.2%, 大于 2 的基本上是 E 类的例子出现的. 这说明尽管山区均匀条件很难满足, 相似理论方法作为经验性的使用, 不会引起较大的误差. 我们应用此方法一共计算了 42 次例子, 并按长度尺度大小分成五种稳定度类, 每类平均参数列于表 5, σ_z 的计算结果见图 6.

表 5　计算 σ_z 的参数表

稳定度类	L(米)	Pasquill 稳定度类[3]	次数	u_* (米/秒)	α	$\bar{u}$ (米/秒)	r
I	−27	B-C	14	0.290	1.8	2.70	0.98
II	−100	C-D	9	0.442	1.8	3.94	0.96
III	−300	D-E	6	0.280	1.8	2.80	0.94
V	100	E-F	8*	0.133	1.8	1.90	0.91
VI	25	F	5	0.086	1.8	1.30	0.87

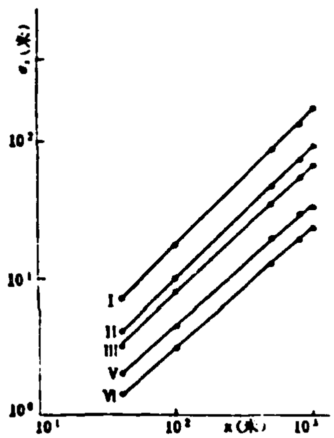

I、II 偏南风.
V、VI 偏北风.
○ 代表计算点值.

图 6　用廓线资料计算的扩散参数 σ_z

六、用铟的浓度分布计算扩散参数

应用实测地面铟浓度资料, 分别计算了水平和垂直扩散参数, 其 σ_y 由

$$\sigma_y^2 = \frac{\Sigma C_i y_i^2}{\Sigma C_i} - \left(\frac{\Sigma C_i y_i}{\Sigma C_i}\right)^2 \tag{17}$$

给出, 式中 C_i 为采样点实测浓度. σ_z 用横向积分浓度方法求出, 其表达式为

$$C_c = \int_{-\infty}^{\infty} C\,dy = \sum_{i=1}^{N} C_i \Delta y = \sqrt{\frac{2}{\pi}}\,\frac{Q}{\sigma_z \bar{u}}\,e^{-\frac{H^2}{2\sigma_z^2}} \tag{18}$$

式中横向积分浓度 C_c, 源强 Q, 平均风速 $\bar{u}$ 和有效源高 H 均为已知量, 则 σ_z 可以求出.

利用上述处理方法, 计算了三次平坦地形偏南风条件的试验资料, 其 σ_z 和 σ_y 的结果见图 7.

对山区的 20 次试验, 由于 800 米以内地形起伏太大, 浓度不满足正态分布, 从 800 米

开始地形起伏较小，其浓度近似满足正态分布．我们只作了 800 和 1500 米两道弧上天气类型属于 E 类（偏北风情况）的 9 次例子的 σ_y 计算，其平均结果也见图 7。

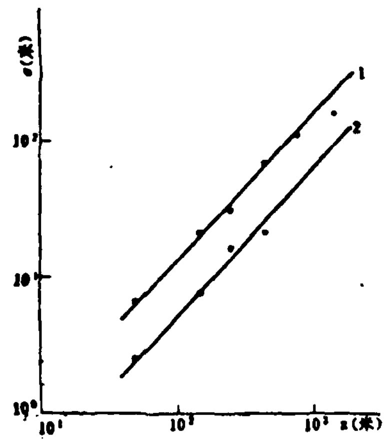

1 平坦地形 σ_y，C 类，3 次平均，偏南风。 } 平均时间 30 分钟
2 平坦地形 σ_z，C 类，3 次平均，偏南风。 }
● 山区 σ_y，E 类，6 次平均，平均时间一小时，偏北风．
○ 代表平坦地形实测值．

图 7　由铟的浓度分布计算扩散参数

七、结果讨论

1. 山区和平原扩散参数比较　　由于山区地形起伏，扩散参数往往比平原要大，为比较起见，我们将从 Pasquill-Gifford[5] 的扩散参数随距离变化曲线内插得到的 σ_y 和 σ_z 为平原情况的代表值，与本文四种方法给出的同一类稳定度的结果进行比较，其 800米处扩散参数的比值列于表 6：

可以看出，在平坦地区作的铟和风向脉动资料计算的 σ_y 和 σ_z 与同一稳定度类的 Pasquill 结果基本上一致．山区与 Pasquill 同类天气比较，山区 σ_z 为平原的 1.9—2.5 倍，山区 σ_y 为平原的 2.0—2.5 倍．因此可以平均地认为，山区的扩散参数为平原扩散参数的

表 6　山区和平原扩散参数比值*

方法 \ 比值 \ 天气类型	C（南风）		E（北风）	
	σ_y/σ_{yp}	σ_z/σ_{zp}	σ_y/σ_y	σ_z/σ_{zp}
铟	1.3平	0.9平	2.4山	—
[illegible]	—	1.9山	—	2.2山
[illegible]	2.5山	2.5山	—	—
脉动法	2.5山 1.1平	— —	2.0山 —	— —

* 凡标有 P 的表示 Pasquill 平原情况的值，下标有"平"的表示平坦地形观测结果，下标有"山"的表示山区结果

2.0—2.5 倍．当风特别大时，地形扰地更强，两者差更大． 如川照相法，在西北大风D类时，山区 σ_y 为平原的 8 倍．因此，从本实验结果，就平均情况，可以近似认为：如果采用平原情况的扩散参数来估计山区的浓度，则比较实际高 4—6 倍． Houind[10] 在山区的某一开阔山地作高架源扩散试验，对D类天气 $C_{山区}/C_{平原}=6.0$，与本文的结果比较一致．同样，Start[11] 在山顶和山谷中分别作扩散试验，中性情况（相当 C-D 类）$C_{山区}/C_{平原}=5$，也和本文结果基本一致．

2. 山区扩散参数与风向关系 由于山区地形粗糙度空间分布的不均匀性，造成扩散参数随气流来向有很大差别．如偏南风时，地形较平坦，偏北风时，上游为高山起伏的地形，这两种地面状况对气流的扰动差别很大． 把图 2a 直线 1、2 和 3、4 作比较可以看出，东北风的 C-D 类比南风的 C 类 σ_y 大将近两倍，在西北大风时就大得更多． 如西北大风时D类的 σ_y 比南风时的 B 类还要大得多，同一稳定度类，可大 4—5 倍．因此，在山区扩散参数的选取中，风向是一个非常重要的因子．

3. 山区近地面层平均风速廓线特征 100 米以下近地面层山区平均风梯度资料分析表明，非中性条件时平均风速廓线可以用对数线性规律逼近，其 α 值比平原小得多，本文平均结果为 1.8±1.15，这地形垂直方向扰动大，造成混合均匀有关． 中性条件基本满足对数分布，其粗糙度长为 0.62 米．

参 考 资 料

[1] 中国科学院冰川冻土沙漠研究所，地面立体摄影测量基础及其应用，1973．

[2] U. S. Atomic Energy Commission, Meteorology and Atomic Energy, 1968.

[3] H. E. Hesketh, Understanding & Controlling Air Pollution, 1972.

[4] J. S. Hay and F. Pasquill, Advances in Geophysics. 1959, 6, P 471.

[5] D. B. Turner, PB 191482, 1970.

[6] T. Sensku, Symposium On Atmospheric Diffusion and Air Pollution, 1974, PP180—183.

[7] K. Takeuchi, *J. Meteor. Soc. Japan*, 1961, 39(6) PP 346—367.

[8] H. A. Panofshy and B. Prasad, *Int. J. Air. Wat. Poll*, 1965, 9(7—8), P419.

[9] A. S. Monin, 同[4], PP331—341.

[10] E. Houind, 同[6], PP214—217.

[11] G. F. Start, 同[6], PP226—232.

ATE
LME